

## Simultaneous Measurements of Visible (400–700 nm) and Infrared (3.4 $\mu\text{m}$ ) $\text{NO}_2$ Absorption

Denis G. Dufour,<sup>\*,†</sup> James R. Drummond,<sup>†</sup> C. Thomas McElroy,<sup>†,‡</sup> Clive Midwinter,<sup>†,‡</sup>  
Peter F. Bernath,<sup>§</sup> Kaley A. Walker,<sup>§</sup> and Caroline Nowlan<sup>†</sup>

Department of Physics, University of Toronto, Toronto, Canada, M5S 1A7, Environment Canada,  
Toronto, Canada, M3H 5T4, and Department of Chemistry, University of Waterloo, Waterloo, Ontario,  
Canada, N2L 3G1

Received: June 2, 2006; In Final Form: September 18, 2006

Laboratory measurements of  $\text{NO}_2$  absorption were obtained in the visible (400–700 nm) and mid-infrared (3.4  $\mu\text{m}$ ) regions simultaneously using SCISAT-1's ACE-FTS (atmospheric chemistry experiment-Fourier transform spectrometer) and MAESTRO (measurement of aerosol extinction in the stratosphere and troposphere retrieved by occultation) spectrometers. An intercomparison of these measurements was used to verify the consistency between the HITRAN 2004 3.4- $\mu\text{m}$  band strengths and the strengths of three different visible cross section data sets. These measurements should be of interest to the remote-sensing community, since  $\text{NO}_2$  measurements obtained by infrared-range instruments are often compared to those obtained by visible-range instruments without accurate knowledge of the consistency between the visible and infrared absorption coefficients. Two significant results were obtained in this study: (1) A 0.5% agreement was found between the HITRAN 2004 line strengths and the Vandaele et al. (Vandaele, A. C.; Hermans, C.; Fally, S.; Carleer, M.; Colin, R.; Mérienne, M.-F.; Jenouvrier, A.; Coquart, B. *J. Geophys. Res.* **2002**, *107* (D18), 4348) temperature-corrected cross sections, and (2) the mean pressure-broadened half-width of  $\text{NO}_2$  by NO in the 3.4- $\mu\text{m}$  band was measured as being  $0.096 \pm 0.001 \text{ cm}^{-1} \text{ atm}^{-1}$ . The latter finding is thought to be unreported by the literature.

### 1. Introduction

Nitrogen dioxide is an important atmospheric compound because of its link to ozone destruction in the stratosphere and its role as a tropospheric pollutant. Accurate remote-sounding measurements of  $\text{NO}_2$  and other atmospheric species are dependent on the certainty to which their spectral line strengths are known. A recent study by Orphal<sup>1</sup> compared the integrated  $\text{NO}_2$  absorption cross sections between 400 and 500 nm for 14 data sets: an average deviation from the mean of  $\pm 1.9\%$  was found. To determine which of these data sets agrees best with currently accepted infrared line parameters, we compared simultaneously measured visible (400–700 nm) and infrared (3.4  $\mu\text{m}$ ) band absorption spectra. These measurements were taken during the preflight testing of the SCISAT-1 spectrometer instruments, ACE-FTS (atmospheric chemistry experiment-Fourier transform spectrometer), and MAESTRO (measurement of aerosol extinction in the stratosphere and troposphere retrieved by occultation).<sup>2</sup> Such measurements are challenging and rarely performed, because of the requirement for a stable, wide-spectral-range source spanning the visible and the mid-infrared and the necessity of using two separate spectrometers to cover this range.

$\text{NO}_2$  amounts, obtained by fitting the 3.4- $\mu\text{m}$  band ACE-FTS measurements using HITRAN 2004 spectral parameters,<sup>3</sup> were compared with simultaneously measured amounts obtained by

MAESTRO. The MAESTRO amounts were derived by fitting the measured spectra using three of the visible cross section data sets examined by Orphal. The Vandaele et al. (1996) data set,<sup>4</sup> obtained using a Fourier transform spectrometer with a resolution of  $0.02 \text{ cm}^{-1}$ , was chosen because its integrated cross section is closest to the average determined by Orphal (the difference is less than 0.5%). The data set reported by Vandaele et al. in 2002,<sup>5</sup> whose integrated cross section is 2% lower than Orphal's average, was chosen because of its high spectral resolution ( $0.1 \text{ cm}^{-1}$ ) and because it contains measurements obtained for a variety of temperature and pressure conditions (220–294 K and 0.001–101.3 kPa, respectively). Optimal cross sections could therefore be calculated to match the temperature of our gas cell. The third data set studied was obtained by Burrows et al. in 1998 using the GOME spectrometer.<sup>6</sup> It has a resolution of about 0.3 nm and was obtained for temperatures between 202 and 293 K. Its integrated cross section between 400 and 500 nm is 3.8% lower than Orphal's average. No particular value was seen in fitting the MAESTRO spectra using all the data sets studied by Orphal, since he had already measured how their integrated cross section strengths differ with respect to each other.

### 2. Experimental Section

The SCISAT-1 satellite was successfully launched on August 12, 2003. Its two instruments, ACE-FTS and MAESTRO, were designed to measure atmospheric extinction spectra during solar occultation events to retrieve vertical profiles of  $\text{O}_3$ ,  $\text{NO}_2$ , and other species relevant to dynamical and chemical processes associated with ozone. The ACE-FTS spectrometer consists of a Michelson interferometer with InSb and HgCdTe (MCT)

\* Author to whom correspondence should be addressed. Telephone: (416) 978-0932. Fax: (416) 978-8905. E-mail: denis@atmosph.physics.utoronto.ca.

<sup>†</sup> University of Toronto.

<sup>‡</sup> Environment Canada.

<sup>§</sup> University of Waterloo.

detectors. It has a spectral range of 750–4400 cm<sup>-1</sup> and a resolution of 0.02 cm<sup>-1</sup>. MAESTRO contains two holographic-grating spectrometers with 1024-pixel detector arrays. The first, labeled “UV”, operates between 270 and 570 nm with a resolution of approximately 1.5 nm, while the second, labeled “vis”, has a spectral range of 525–1040 nm and a resolution of approximately 2.5 nm.

For the prelaunch instrument characterization at the University of Toronto Instrument Characterization Facility (ICF) in February and March 2003, the two instruments were mounted in a vacuum chamber on a replica of the SCISAT-1 base plate. A solar simulator source was constructed which enabled simultaneous gas absorption measurements with both instruments. It consisted of a 1000 W quartz halogen lamp and a 3000 K blackbody source, whose beams were merged into a common field of view by using a germanium beam splitter. This apparatus has been described in more detail in a previous paper.<sup>7</sup> Light from the solar simulator entered the vacuum chamber through a BaF<sub>2</sub> window. A 20-cm-long gas stainless steel gas cell with wedged BaF<sub>2</sub> windows was positioned between the solar simulator source and the vacuum chamber. It was filled by evaporating gas out of a cylinder of pure liquid NO<sub>2</sub> (exact purity unknown) obtained from the Meteorological Service of Canada. Following each full-cell measurement, the cell was removed, evacuated, and then repositioned for an empty-cell measurement. The photodissociation of NO<sub>2</sub> into NO was observed and characterized by measuring the decrease in NO<sub>2</sub> amount and the increase in NO amount as a function of time. NO amounts were obtained by fitting fundamental band (1700–2000 cm<sup>-1</sup>) spectra measured by ACE-FTS using HITRAN 2004 line data. A significant amount of N<sub>2</sub>O<sub>4</sub> was present in the cell because of the high concentration of NO<sub>2</sub>. Since N<sub>2</sub>O<sub>4</sub> can cause interference in the NO<sub>2</sub> spectrum at wavelengths below 450 nm, the amount of N<sub>2</sub>O<sub>4</sub> as a function of time was determined from ACE-FTS measurements by using the temperature-dependent integrated  $\nu_{11}$  band intensities reported by Hurtmans et al.<sup>8</sup> The effect of N<sub>2</sub>O<sub>4</sub> absorption in the MAESTRO spectral range could then be determined using published N<sub>2</sub>O<sub>4</sub> visible cross sections.

### 3. Spectral Fitting

The amount of NO<sub>2</sub> in the cell was obtained by iterative least-squares fitting of measured full-cell spectra with modeled full-cell spectra. The modeled full-cell spectra were obtained by using published spectral line data, best-guess absorber amount and optical frequency dispersion parameters, and measured gas cell temperature and instrument line shapes to generate effective transmission spectra. The effective transmissions were then converted to modeled full-cell spectra by multiplication with reference-measured empty-cell spectra. For ACE-FTS, the modeled spectra were generated at a wavenumber grid resolution of 0.001 cm<sup>-1</sup> by using the GENSPECT line-by-line spectral toolbox.<sup>9</sup> For MAESTRO, the modeled transmissions were calculated using Beer's Law with published cross section data. The calculation was done on a wavelength grid corresponding to the smallest wavelength interval in the cross-sectional data set. The spectral resolution of the two Vandaele et al. data sets are unnecessarily fine, however, so the data was decimated to a coarser scale by a factor of 20. A more detailed description of the fitting procedure has been published in a previous paper.<sup>7</sup>

An alternate fitting technique, equivalent in principle to differential optical absorption spectroscopy (DOAS),<sup>10</sup> was developed to fit the infrared NO<sub>2</sub> spectra. Our objective was to see if we could eliminate the need for reference empty-cell

spectra measurements when fitting the ACE-FTS NO<sub>2</sub> spectra. The high-frequency spectral content of the NO<sub>2</sub> absorption lines was separated from the low-frequency content of the baseline solar simulator spectrum by multiplying the fast Fourier transform (FFT) of the full-cell spectra with a modified step function at 2.75 cm<sup>-1</sup>. The step function was rounded by using a sine function to minimize Gibb's modulation. Low-pass spectra were then obtained by performing an inverse FFT of the low-pass FFT. The ratio of the measured full-cell spectra divided by its low-pass component was then fitted with the ratio of the modeled effective transmission divided by its low-pass component, using the same least-squares fitting algorithm used for the “regular” fitting method.

Both fitting methods yielded similar NO<sub>2</sub> amounts (within 1%), demonstrating that the FFT-filtering technique is a valid analysis method. However, good discrimination between the frequency content of the spectral lines and the baseline is required to obtain accurate results with this technique. When it was used to fit 4.8- $\mu$ m band O<sub>3</sub> measurements obtained with the same apparatus, the lower frequency content of the O<sub>3</sub> spectral lines in comparison with the NO<sub>2</sub> lines resulted in poor fitting residuals.

### 4. Results

The intercomparison of NO<sub>2</sub> amounts obtained by MAESTRO and ACE-FTS for a gas cell filled with 10 Torr of undiluted NO<sub>2</sub> is presented here. Measurements were also taken with the gas cell filled to other pressures and mixes of NO<sub>2</sub> with air, but these were not analyzed in depth because of excessive baseline drifts. “Baseline drift” is caused by irregular changes in the solar simulator illumination signal recorded by the two spectrometers, occurring on the time scale of hours. These drifts, resulting from thermal etaloning drifts for MAESTRO and detector ice buildup for ACE-FTS, were examined by looking at changes in signal intensity between full-cell and reference empty-cell measurements in regions with no absorption lines. The baseline drift for the 10 Torr undiluted NO<sub>2</sub> data set was quite small, less than 0.01% of the signal intensity in the MAESTRO region. This is comparable to the magnitude of the short time scale baseline jumps caused by chaotic thermal fluctuations of the solar simulator sources. For the other data sets, baseline drift biases of about 0.05% of the signal magnitude were measured, which would result in significant errors in fitted NO<sub>2</sub> amounts.

For the 10 Torr undiluted NO<sub>2</sub> data set, a set of full-cell measurements was followed by a set of empty-cell measurements 1 h later. In each 11-min-long set, MAESTRO measured 170 spectra co-added in 34 groups of 5, while ACE-FTS measured 300 spectra co-added in 15 groups of 20. The ACE-FTS and MAESTRO empty-cell measurements were averaged to generate baseline reference spectra. A typical ACE-FTS full-cell spectrum is shown in Figure 1, with the least-squares fit residual shown on the bottom. Figures 2 and 3 show typical full-cell spectra recorded by MAESTRO's UV and vis spectrometers, respectively, with the reference empty-cell spectra on top. Fitting residuals from the best fit obtained using Vandaele et al. (2002) cross sections adjusted to the measured gas cell temperature of 303 K are shown on the bottom. The small oscillations in the residuals are thought to be mostly due to uncertainties in the change in the instrument line shape with wavelength. These oscillations are larger for the UV spectrometer (Figure 2) than the vis spectrometer (Figure 3) because of increased line shape uncertainty. While three laser wavelengths were used to probe the variation of line shape with wavelength in the vis range, only one line at 532 nm, near the edge of the

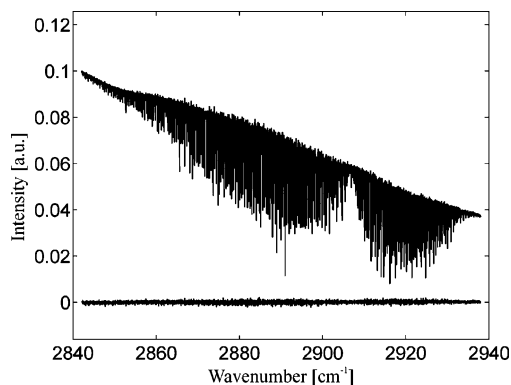


**Figure 1.** Typical ACE-FTS full-cell  $\text{NO}_2$  absorption spectrum for the 10 Torr data set. The residual from the best fit using HITRAN 2004 data is shown on the bottom.

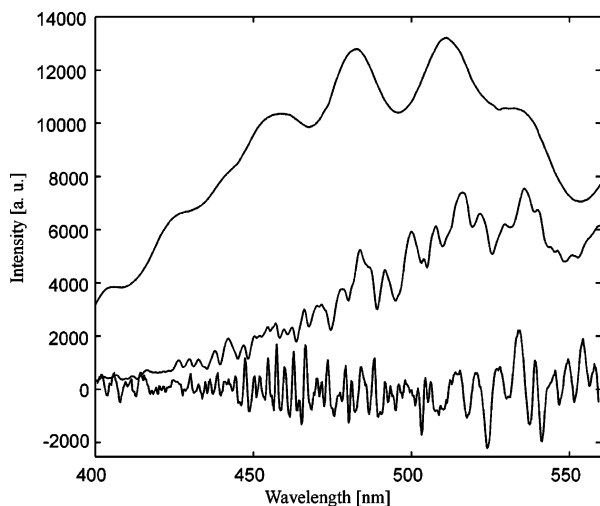


**Figure 2.** Typical MAESTRO full-cell (middle curve) and empty-cell (top curve)  $\text{NO}_2$  spectra measured by the UV spectrometer for the 10 Torr data set. The residual from the best fit using the Vandaele et al. (2002) data set at a temperature of 303 K, multiplied by  $10\times$ , is shown on the bottom.

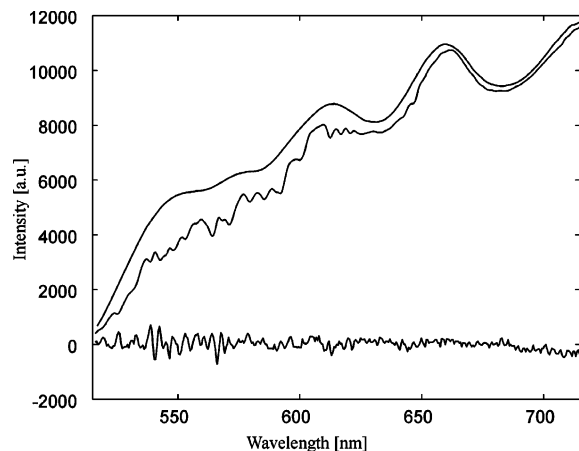


**Figure 3.** Typical MAESTRO full-cell (middle curve) and empty-cell (top curve)  $\text{NO}_2$  spectra measured by the vis spectrometer for the 10 Torr data set. The residual from the best fit using the Vandaele et al. (2002) data set at a temperature of 303 K, multiplied by  $10\times$ , is shown on the bottom.

spectral range, was available for the UV spectrometer. Fitting residuals obtained when using this line shape show it was clearly too narrow for the rest of the spectral range, and therefore a best-fit line shape width scaling parameter of 1.6 was obtained to minimize the least-squares fit of the UV spectra. Since the

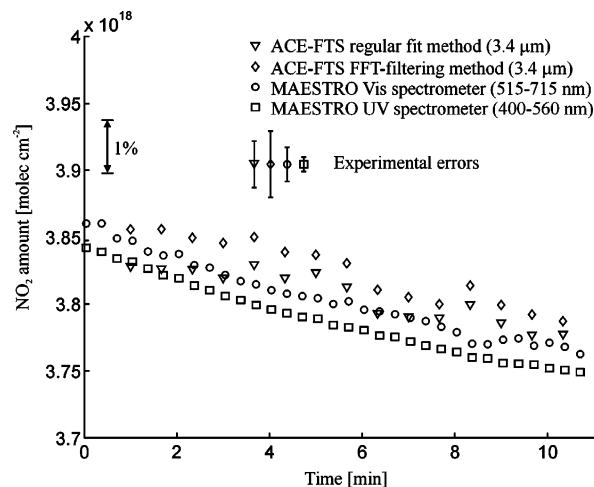


**Figure 4.** Intercomparison of fitted  $\text{NO}_2$  amounts as function of time. ACE-FTS amounts were obtained using HITRAN 2004 data. MAESTRO amounts were obtained using Vandaele et al. temperature-dependent cross sections (2002) at 303 K. ACE-FTS results using both the standard and FFT-filtered fitting methods are shown by triangles and diamonds, respectively. MAESTRO results using both the UV and vis spectrometers are shown by squares and circles, respectively. The errors bars represent the estimated experimental uncertainties, as shown in Table 2. These uncertainties do not include errors in cross-sectional and line data.

**TABLE 1: Mean  $\text{NO}_2$  Amounts Obtained with ACE-FTS and MAESTRO**

	mean fit amount ( $10^{18}$ molec $\text{cm}^{-2}$ )	percent difference relative to ACE-FTS mean fit amount (regular fit method)
ACE-FTS		
regular fit method	$3.806 \pm 0.018$	0%
baseline-filtering fit method	$3.825 \pm 0.025$	0.50%
MAESTRO		
Burrows et al. (1998) UV	$3.8739 \pm 0.0054$	1.79%
Burrows et al. (1998) vis	$3.900 \pm 0.013$	2.46%
Vandaele et al. (1996) UV	$3.8272 \pm 0.0054$	0.56%
Vandaele et al. (1996) vis	$3.884 \pm 0.013$	2.05%
Vandaele et al. (2002) UV	$3.7875 \pm 0.0054$	-0.48%
Vandaele et al. (2002) vis	$3.8033 \pm 0.013$	-0.07%

true line shape width changes with wavelength, oscillations in the fitting residual are seen.

The intercomparison of  $\text{NO}_2$  amounts measured by MAESTRO and ACE-FTS during the 11-min period is shown in Figure 4. MAESTRO amounts obtained using both the UV and vis spectrometers with the Vandaele et al. (2002) temperature-adjusted cross sections are shown. For ACE-FTS, amounts fitted using the regular fit method and the FFT-filtered fit method are shown. The graph suggests a good agreement, within 0.5%, between the strengths of the Vandaele et al. (2002) cross sections and the HITRAN 2004 3.4- $\mu\text{m}$  band strengths. Larger discrepancies were seen when using the Vandaele et al. (1996) and the Burrows et al. cross sections, as shown in Table 1. A bias of approximately 0.5% was measured between the ACE-FTS amounts obtained using the two fit methods. Since this is smaller than the measurement uncertainty, the FFT-filtering method seems to produce accurate results. There is also a bias of approximately 0.4% between MAESTRO amounts measured with the UV and vis spectrometers. Interestingly, a different UV-vis bias, 1.5%, is obtained when using the Vandaele et al. (1996) cross sections instead, which suggests that the biases are inherent in the published data. The interference by  $\text{N}_2\text{O}_4$  in the visible was modeled using the cross-sectional data of Bass

**TABLE 2: Uncertainty Sources for MAESTRO and ACE-FTS Fitted NO<sub>2</sub> Amounts**

uncertainty source	MAESTRO UV	MAESTRO vis	ACE-FTS regular method	ACE-FTS FFT-filtered method
baseline fluctuations	0.08%	0.28%	0.38%	0.61%
wavelength dispersion	0.10%	0.016%	0.01%	0.01%
gas cell temperature	0.04%	0.07%	0.15%	0.08%
instrument line shape	0.05%	0.16%		
foreign-broadened half-widths			0.21%	0.21%
total	0.14%	0.33%	0.46%	0.65%

et al.<sup>11</sup> and Harwood and Jones,<sup>12</sup> combined with the N<sub>2</sub>O<sub>4</sub> pressure measured using the infrared  $\nu_{11}$  band. Because of the small magnitude of the modeled N<sub>2</sub>O<sub>4</sub> absorption above the peak ( $\sim 1\%$  at 430 nm using the Harwood and Jones 253 K data), the impact of N<sub>2</sub>O<sub>4</sub> interference on NO<sub>2</sub> amounts obtained by spectral fitting at wavelengths greater than 400 nm should be negligible.

The infrared NO<sub>2</sub> spectra are much more sensitive to pressure-broadening effects than the visible spectra. The pressure-broadened line widths modeled using HITRAN 2004 half-width parameters were obviously narrower than the ACE-FTS measurements. The missing broadening was thought to be due to the presence of NO and N<sub>2</sub>O<sub>4</sub> in the cell, for which HITRAN 2004 does not provide pressure-broadening parameters. Assuming no other impurities of significance in the cell, and using the mean foreign-broadening half-width of NO<sub>2</sub> by N<sub>2</sub>O<sub>4</sub> as reported by Dana et al.<sup>13</sup> with the mean measured partial pressures of NO and N<sub>2</sub>O<sub>4</sub> ( $660 \pm 4$  Pa and  $20 \pm 4$  Pa, respectively), an estimate of the foreign broadening width of NO<sub>2</sub> by NO was derived. The calculated value of  $0.096 \pm 0.001$  cm<sup>-1</sup> atm<sup>-1</sup> is very close to the mean NO<sub>2</sub> self-broadening half-width reported by Dana et al.,  $0.0935 \pm 0.0093$  cm<sup>-1</sup> atm<sup>-1</sup>, and is higher than their reported air-broadening widths, which vary between 0.06 and 0.08 cm<sup>-1</sup> atm<sup>-1</sup>.

## 5. Uncertainty Analysis

The effects of several independent sources of uncertainty were combined to determine the uncertainty in the NO<sub>2</sub> amounts measured by ACE-FTS and MAESTRO. For MAESTRO, the effects of uncertainty in gas cell temperature, baseline stability, wavelength dispersion parameters, and instrument line shape on the fitted NO<sub>2</sub> amounts were estimated. The effect of temperature uncertainty on fitted amounts was calculated by considering the influence of temperature on cross sections as modeled by Vandaele et al. (2002), combined with the estimated uncertainty in the measured gas cell temperature,  $\pm 1$  K. Analysis of the empty-cell spectra showed the presence of short time scale ( $\sim 1$  s) baseline jumps, thought to be caused by chaotic thermal fluctuations of the solar simulator source. To estimate the uncertainty due to these fluctuations, the standard deviation of the difference between individual NO<sub>2</sub> amounts and the second-order polynomial fit of the amount decrease as function of time was calculated. The instrument line shape uncertainty was estimated by measuring the slight changes in the line shape obtained using lasers of different wavelengths. As shown in Table 2, the effect of these error sources on the fitted amounts is different for spectra measured with the UV and vis spectrometers, with the UV showing the smaller total uncertainty.

Similar calculations were undertaken to determine the effect of these error sources on ACE-FTS fitted amounts. One major difference is the inclusion of uncertainty in the magnitude of the pressure broadening because of NO and N<sub>2</sub>O<sub>4</sub> in the cell. This uncertainty was estimated by calculating the standard deviation of the foreign-broadened half-widths fitted for each spectrum in the full-cell set. The uncertainty in fitted NO<sub>2</sub>

amounts obtained by the two ACE-FTS fitting methods is shown alongside the MAESTRO uncertainties in Table 2.

## 6. Conclusions

The intercomparison of simultaneously obtained NO<sub>2</sub> absorption spectra in the visible (400–700 nm) and infrared (3.4  $\mu$ m) spectral regions was performed. Results show a good agreement, within 0.5%, between the 3.4- $\mu$ m region strengths reported in HITRAN 2004 and the strengths of the temperature-dependent visible cross sections reported by Vandaele et al. (2002). It must be cautioned that this study is a comparison of relative strengths and makes no claim regarding the absolute accuracies of these datasets. The only other NO<sub>2</sub> visible–infrared intercomparison study known to the authors was performed by Flaud and Orphal.<sup>14</sup> They compared the infrared absorption by NO<sub>2</sub> in the 3.4- $\mu$ m region using a difference-frequency laser source with absorption in the 360–440 nm region using a Hg lamp source. A difference of about 5% between Orphal's recommended ultraviolet–visible cross sections and the  $\nu_1 + \nu_3$  band that makes up the majority of the 3.4- $\mu$ m region absorption lines was reported.

In addition to the infrared-visible intercomparison, the mean pressure broadening half-width of NO<sub>2</sub> by NO in the 3.4- $\mu$ m band was determined as being  $0.096 \pm 0.001$  cm<sup>-1</sup> atm<sup>-1</sup>. This measurement is thought to be unreported in the literature. The alternate DOAS-related fitting technique which was used to fit ACE-FTS NO<sub>2</sub> spectra without need of a reference empty-cell measurement yielded NO<sub>2</sub> amounts close to those obtained using the regular method (0.5% mean difference). This method could prove useful for future infrared absorption measurements where no background reference measurements are available and the frequency content of the spectral lines is sufficiently separated from that of the background.

**Acknowledgment.** This research was made possible thanks to funding from the Canadian Space Agency (CSA), the Natural Sciences and Engineering Research Council of Canada (NSERC), and the Canadian Foundation for Climate and Atmospheric Sciences (CFCAS). Support at the University of Waterloo was also provided by the NSERC-Bomem-CSA-MSU Industrial Research Chair in Fourier Transform Spectroscopy.

## References and Notes

- Orphal, J. A Critical Review of the Absorption Cross Sections of O<sub>3</sub> and NO<sub>2</sub> in the Ultraviolet and Visible. *J. Photochem. Photobiol., A: Chem.* **2003**, *157*, 185–209.
- Bernath, P. F.; McElroy, C. T.; Abrams, M. C.; Boone, C. D.; Butler, M.; Camy-Peyret, C.; Carleer, M.; Clerbaux, C.; Coheur, P.-F.; Colin, R.; DeCola, P.; De Mazière, M.; Drummond, J. R.; Dufour, D.; Evans, W. F. J.; Fast, H.; Fussen, D.; Gilbert, K.; Jennings, D. E.; Llewellyn, E. J.; Lowe, R. P.; Mahieu, E.; McConnell, J. C.; McHugh, M.; McLeod, S. D.; Michaud, R.; Midwinter, C.; Nassar, R.; Nichitiu, F.; Nowlan, C.; Rinsland, C. P.; Rochon, Y. J.; Rowlands, N.; Semeniuk, K.; Simon, P.; Skelton, R.; Sloan, K. J.; Soucy, M.-A.; Strong, K.; Tremblay, P.; Turnbull, D.; Walker, K. A.; Walkty, I.; Wardle, D. A.; Wehrle, V.; Zander, R.; Zou, J. Atmospheric Chemistry Experiment (ACE): Mission Overview. *Geophys. Res. Lett.* **2005**, *32*, L15S01.

- (3) Rothman, L. S.; Jacquemart, D.; Barbe, A.; Chris Benner, D.; Birk, M.; Brown, L. R.; Carleer, M. R.; Chackerian, C., Jr.; Chance, K.; Coudert, L. H.; Dana, V.; Devi, V. M.; Flaud, J.-M.; Gamache, R. R.; Goldman, A.; Hartmann, J.-M.; Jucks, K. W.; Maki, A. G.; Mandin, J.-Y.; Massie, S. T.; Orphal, J.; Perrin, A.; Rinsland, C. P.; Smith, M. A. H.; Tennyson, J.; Tolchenov, R. N.; Toth, R. A.; Vander Auwera, J.; Varanasi, P.; Wagner, G. The HITRAN 2004 Molecular Spectroscopic Database. *J. Quant. Spectrosc. Radiat. Transfer* **2005**, *96*, 139–204.
- (4) Vandaele, A. C.; Hermans, C.; Simon, P. C.; Van Roozendael, M.; Guilmot, J. M.; Carleer, M.; Colin, R. Fourier Transform Measurement of NO<sub>2</sub> Absorption Cross Sections in the Visible Range at Room Temperature. *J. Atmos. Chem.* **1996**, *25*, 289–305.
- (5) Vandaele, A. C.; Hermans, C.; Fally, S.; Carleer, M.; Colin, R.; Mérienne, M.-F.; Jenouvrier, A.; Coquart, B. High-resolution Fourier Transform Measurement of the NO<sub>2</sub> Visible and Near-infrared Cross-sections: Temperature and Pressure Effects. *J. Geophys. Res.* **2002**, *107* (D18), 4348.
- (6) Burrows, J. P.; Dehn, A.; Deters, B.; Himmelmann, S.; Richter, A.; Voigt, S.; Orphal, J. Atmospheric Remote-sensing Reference Data from GOME: Part I. Temperature-dependent Absorption Cross-sections of NO<sub>2</sub> in the 231–794 nm Range. *J. Quant. Spectrosc. Radiat. Transfer* **1998**, *60* (6), 1025–1031.
- (7) Dufour, D. G.; Drummond, J. R.; McElroy, C. T.; Midwinter, C.; Bernath, P. F.; Walker, K. A.; Evans, W. F. J.; Puckrin, E.; Nowlan, C. Intercomparison of Simultaneously Obtained Infrared (4.8 μm) and Visible (515–715 nm) Ozone Spectra Using ACE-FTS and MAESTRO. *J. Phys. Chem. A* **2005**, *109*, 8760–8764.
- (8) Hurtmans, D.; Herman, M.; Vander Auwera, J. Integrated Band Intensities of N<sub>2</sub>O<sub>4</sub> in the Infrared Range. *J. Quant. Spectrosc. Radiat. Transfer* **1993**, *50* (6), 595.
- (9) Quine, B. M.; Drummond, J. R. GENSPECT: A Line-by-Line Code with Selectable Interpolation Error Tolerance. *J. Quant. Spectrosc. Radiat. Transfer* **2002**, *74*, 147–165.
- (10) Mellqvist, J.; Rosén, A. DOAS for Flue Gas Monitoring – I. Temperature Effects in the U.V./Visible Absorption Spectra of NO, NO<sub>2</sub>, SO<sub>2</sub> and NH<sub>3</sub>. *J. Quant. Spectrosc. Radiat. Transfer* **1996**, *56* (2), 187–208.
- (11) Bass, A. M.; Ledford, A. E., Jr.; Laufer, A. H. Extinction Coefficients of NO<sub>2</sub> and N<sub>2</sub>O<sub>4</sub>. *J. Res. Natl. Bur. Stand. Sect A* **1976**, *80*, 143–166.
- (12) Harwood, M. H.; Jones, R. L. Temperature Dependent Ultraviolet-visible Absorption Cross-sections of NO<sub>2</sub> and N<sub>2</sub>O<sub>4</sub>: Low-temperature Measurements of the Equilibrium Constant for 2NO<sub>2</sub> ↔ N<sub>2</sub>O<sub>4</sub>. *J. Geophys. Res.* **1994**, *99* (D11), 22955.
- (13) Dana, V.; Mandin, J.-Y.; Allout, M.-Y.; Perrin, A.; Régalia, L.; Barbe, A.; Plateaux, J.-J.; Thomas, X. Broadening parameters of NO<sub>2</sub> lines in the 3.4 μm spectral region. *J. Quant. Spectrosc. Radiat. Transfer* **1997**, *57* (4), 445–457.
- (14) Flaud, P.-M.; Orphal, J. *Intercomparison of the Ultraviolet–Visible and Mid-Infrared Absorption Coefficients of Nitrogen Dioxide, NO<sub>2</sub>*, 19th Colloquium on High-Resolution Molecular Spectroscopy, Salamanca, Spain, 2005; Abstract P273.